

Supplementary Information for

**Targeting PKMYT1 enhances antitumor immune responses in
castration-resistant prostate cancer**

Lin Gao^{1,2}, Baozhen Wang¹, Hui Liu³, Ping Liu¹, Long Liu³, Jingying Han¹, Xin Wang¹, Baokai Dou⁴, Wenyao Liu³, Xinpei Wang¹, Feifei Sun¹, Tingting Feng¹, Ru Zhao³, Weiwen Chen², Jing Hu³ ✉ and Bo Han^{1,3,5} ✉

Corresponding author

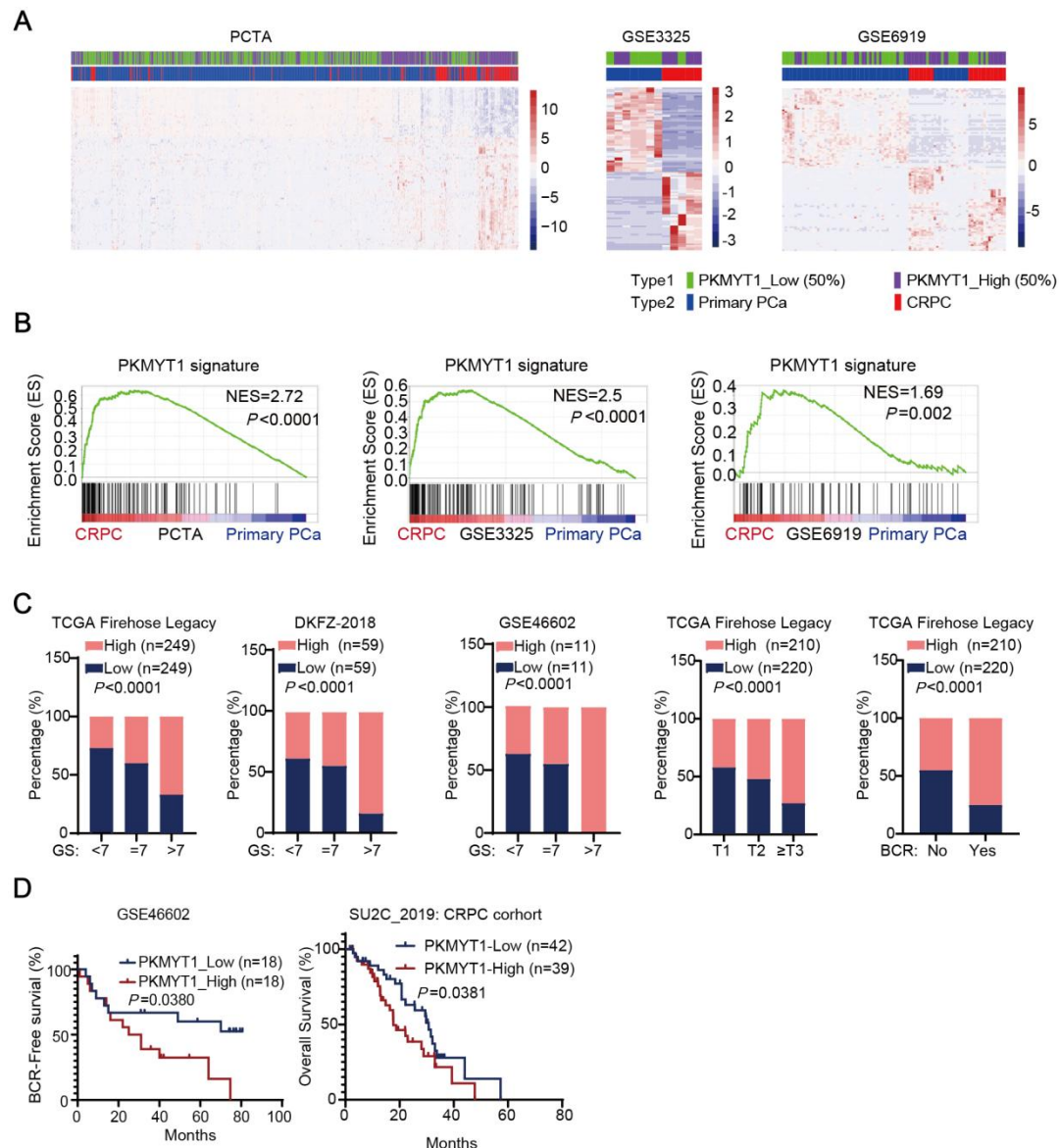
Jing Hu, Email: 201420420@mail.sdu.edu.cn

Bo Han, Email: boh@sdu.edu.cn

The PDF file includes:

Supplementary Figure 1 to 13

Supplementary Table 1 to 4



Supplementary Fig.1 PKMYT1 expression is elevated in CRPC and is related with the progression of PCa.

A. Unsupervised clustering analyses of PCTA, GSE3325, and GSE6919 datasets based on differential expression genes of primary PCa and CRPC tissues. Patients' status were shown in the annotation column. Patients were categorized according to PKMYT1 expression or PCa risk assessment. Green: patients with low PKMYT1 expression (50% cutoff); Purple: patients with high PKMYT1 expression (50% cutoff); Blue: patients with primary PCa (Primary PCa); Red: patients with CRPC.

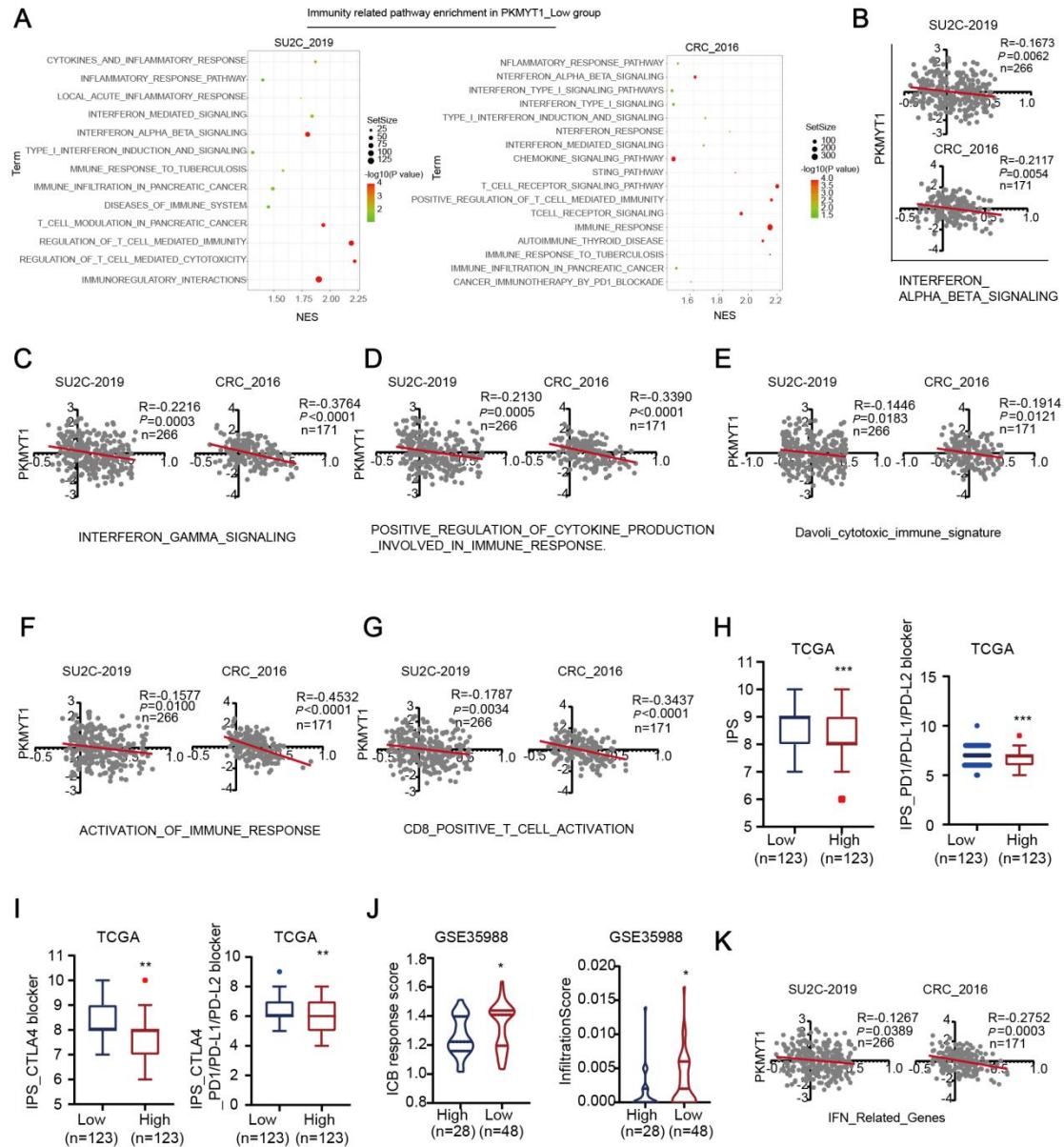
B. Enrichment of PKMYT1 signatures analyzed by GSEA. GSEA analysis was performed to determine the enrichment of PKMYT1 related gene sets in gene expression dataset profiling CRPC and primary PCa in indicated datasets.

C. The relationship between PKMYT1 expression and gleason score, different TNM

stages and biochemical recurrence in indicated datasets.

D. Kaplan–Meier survival analysis of PCa cases from GSE46602 and SU2C-2019. PCa cases in GSE46602 and SU2C-2019 datasets were stratified based on PKMYT1 expression levels, and analyzed for disease-free survival. The P values for Kaplan-Meier curves were determined using a log-rank test.

$*P < 0.05$, $**P < 0.01$, $***P < 0.001$.



Supplementary Fig.2 PKMYT1 expression is associated with type I and II interferon signaling and ICB response in CRPC.

A. Immune related signatures enriched in CRPC cases with PKMYT1 different expression. Immune related signatures download from WP pathway, REACTOME and KEGG were analyzed and shown in bubble plot.

B-G. The relationship between interferon-alpha-beta signaling, interferon-gamma signaling, cytokine production involved in immune response, cytotoxic-immune signature, activation of immune response, CD8 positive T cell activation and PKMYT1 expression in CRPC cases from SU2C-2019 and CRC-2016 datasets. Gene sets from Molecular Signatures Database v7.4 (MSigDB, <https://www.gsea-msigdb.org/gsea/msigdb>) was performed ssGSEA function from GSVA package 1.38.2 to estimates pathway enrichment scores, then enrichment

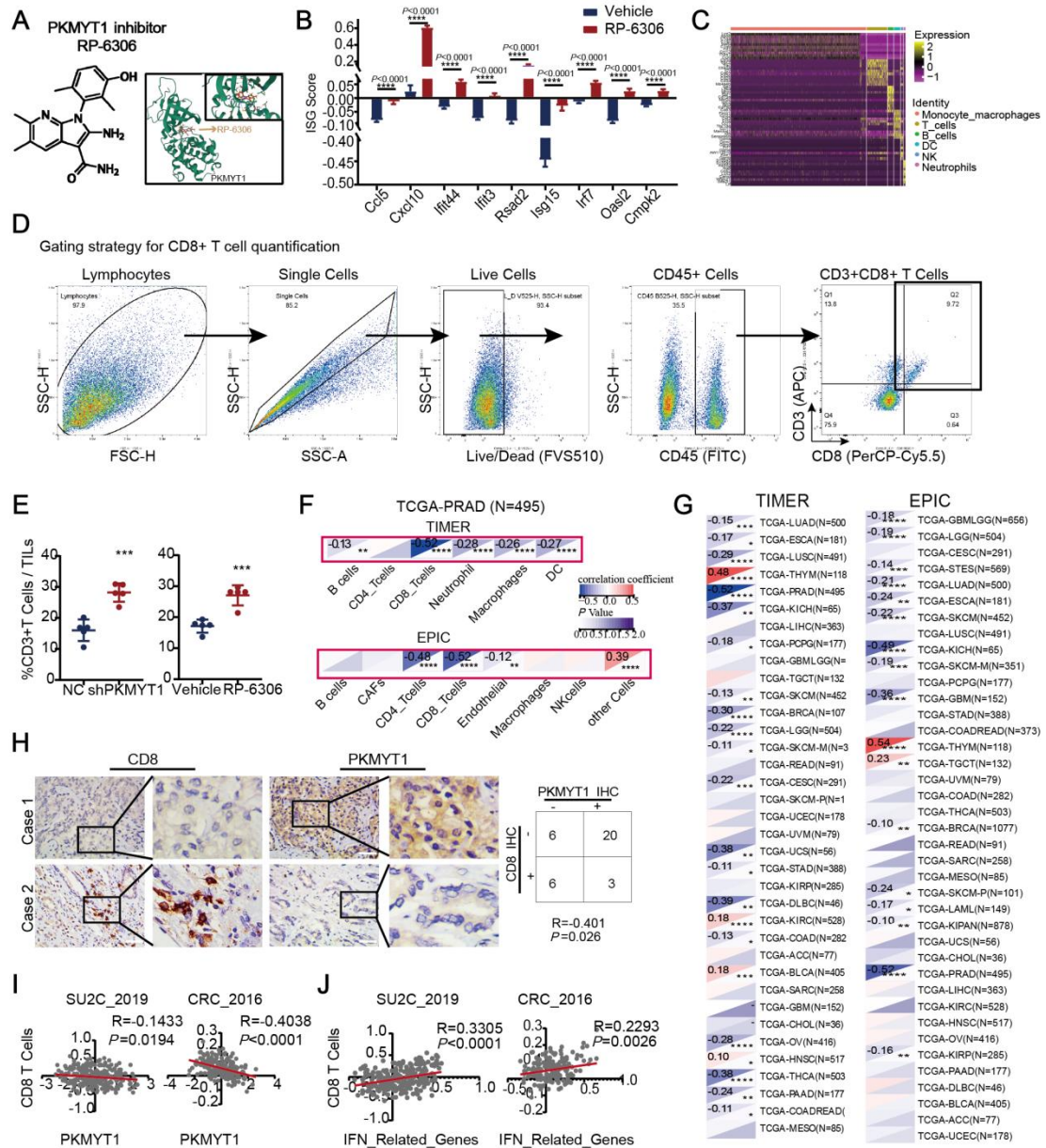
scores were performed Z score normalization cross all samples. Correlation analysis between normalized gene expression and normalized single sample gene set enrichment scores was performed.

H-I. The relationship between IPS and PKMYT1 expression levels in PCa cases. The IPS, IPS-PD1/PD-L1/PD-L2 and IPS-CTLA4 were evaluated in TCIA database (<https://tcia.at/home>).

J. The relationship between of ICB response score and PKMYT1 expression in GSE35988 analyzed by immuneAI.

K. The relationship between IFN signature and PKMYT1 expression in CRPC cases from SU2C-2019 and CRC-2016 datasets.

$*P < 0.05$, $**P < 0.01$, $***P < 0.001$, $****P < 0.0001$.



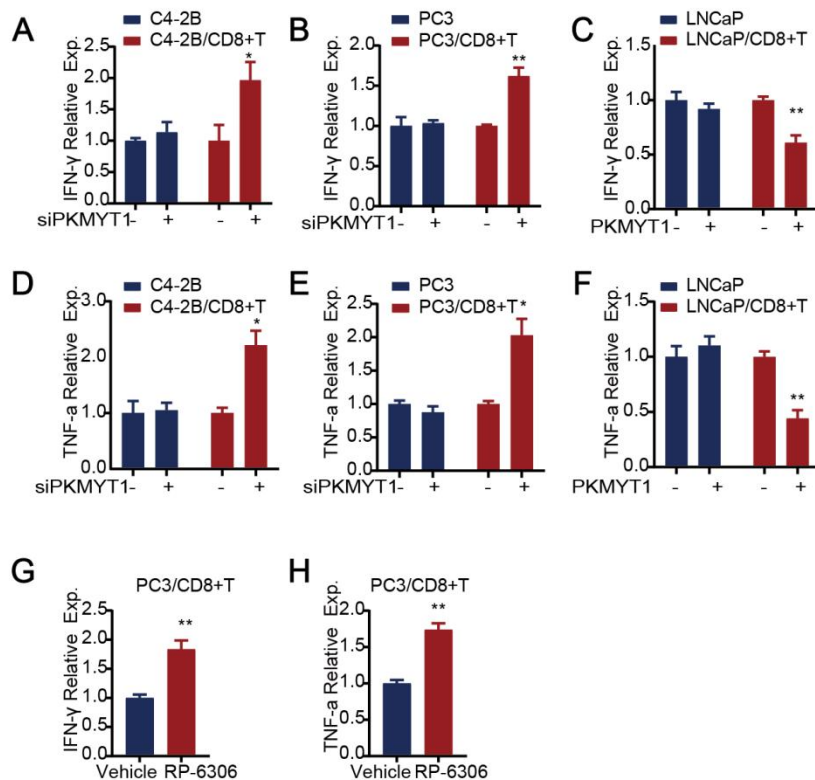
Supplementary Fig.3 Targeting PKMYT1 promotes CD8+ T infiltration.

- The structure of RP-6306.
- ISGs score in RM-1 tumors with indicated treatment analyzed by scRNA-seq.
- The heatmap of immune cells in RM-1 tumors.
- Gating strategy for CD8+ T cell quantification.
- The percentage of CD3+ T cells in CD45+ cells analyzed by flow-cytometry.
- The relationship between immune cell infiltration and PKMYT1 expression levels in PCa analyzed by TIMER and EPIC database.
- The relationship between CD8+ T cell infiltration and PKMYT1 expression in pan-cancer analyzed by TIMER and EPIC database.
- Representative IHC images and quantitative analysis for PKMYT1 and CD8 expression in PCa cases in Qilu hospital. Contingency table for PKMYT1 expression

status by IHC in CRPC cases in Qilu hospital. Scale bars, 50 μ m.

I-J. The relationship between CD8⁺ T cell infiltration and PKMYT1, IFN-related genes expression in CRPC cases from SU2C-2019 and CRC-2016 datasets. Immune cell marker genes list was performed ssGSEA function from GSVA package 1.38.2 to estimates immune cell enrichment scores, then enrichment scores were performed Z score normalization cross all samples. Correlation analysis between normalized gene expression and normalized single sample gene set enrichment scores was performed.

* $P < 0.05$, ** $P < 0.01$, *** $P < 0.001$, **** $P < 0.0001$.

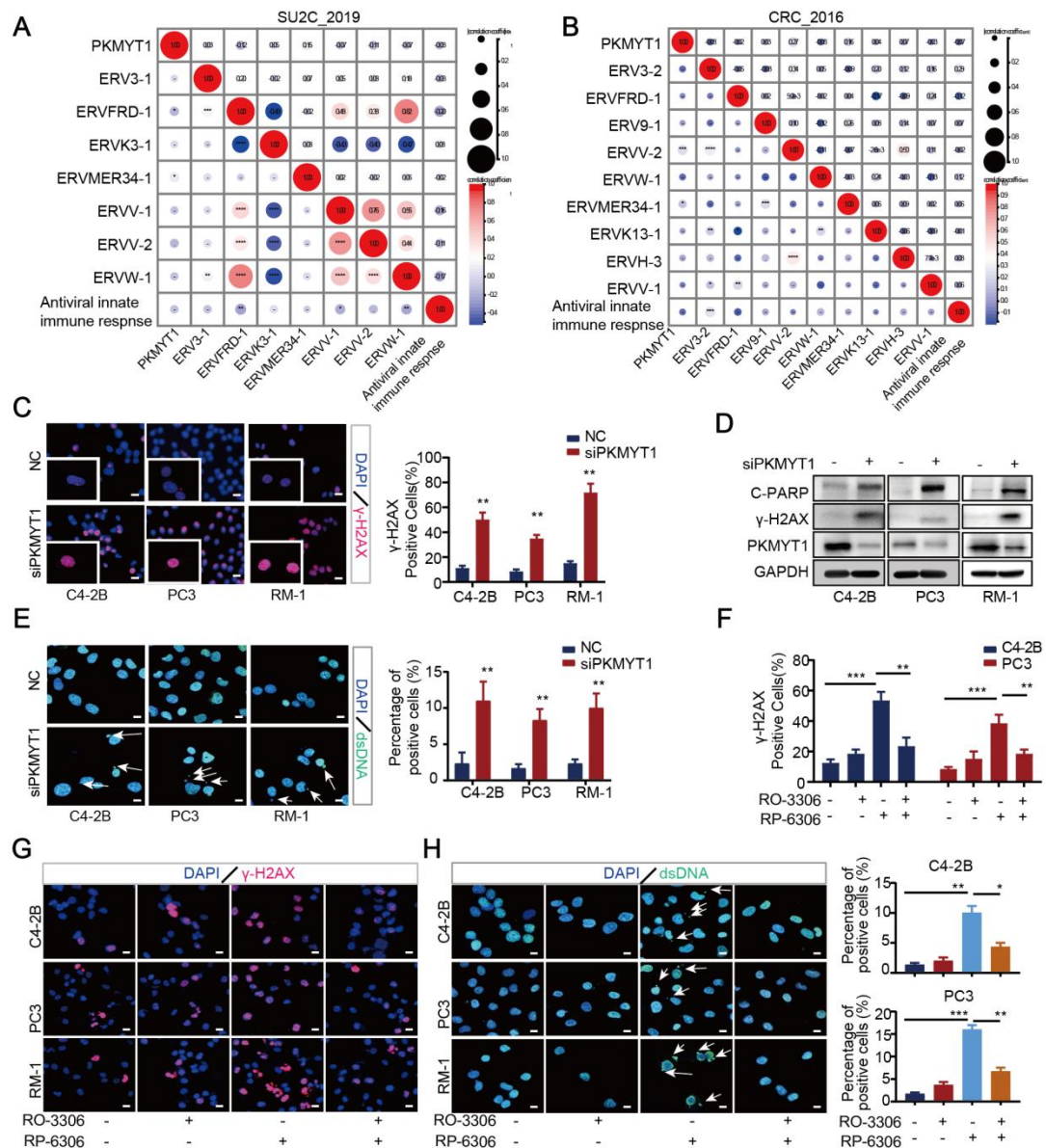


Supplementary Fig.4 Targeting PKMYT1 promotes CD8+ T cell activation.

A-F. IFN- γ and TNF- α levels analyzed by cytokine ELISAs. C4-2B and PC3 cells transfected siPKMYT1 while LNCaP cells transfected PKMYT1, were cocultured with CD8+ T cells for 24h. Cocultured media were analyzed for IFN- γ and TNF- α . The error bars indicate the mean \pm SEM of three independent assays (student *t* test).

G-H. IFN- γ and TNF- α levels analyzed by cytokine ELISAs. PC3 cells treated with 500nM RP-6306, were cocultured with CD8+ T cells for 24h. Cocultured media were analyzed for IFN- γ and TNF- α . The error bars indicate the mean \pm SEM of three independent assays (student *t* test).

P* < 0.05, *P* < 0.01.



Supplementary Fig.5 Targeting PKMYT1 increased DNA damages accumulation and cytoplasmic dsDNA levels.

A-B. The relationship between ERV related genes and PKMYT1 expression in CRPC cases from SU2C-2019 and CRC-2016 datasets.

C. IF staining analysis of γ -H2AX expression in PCa cells with indicated transfection. Percentage of γ -H2AX positive cells was shown in right panel. Scale bars, 20 μ m.

D. Western blot analysis of C-PARP and γ -H2AX expression in PCa cells with PKMYT1 knockdown.

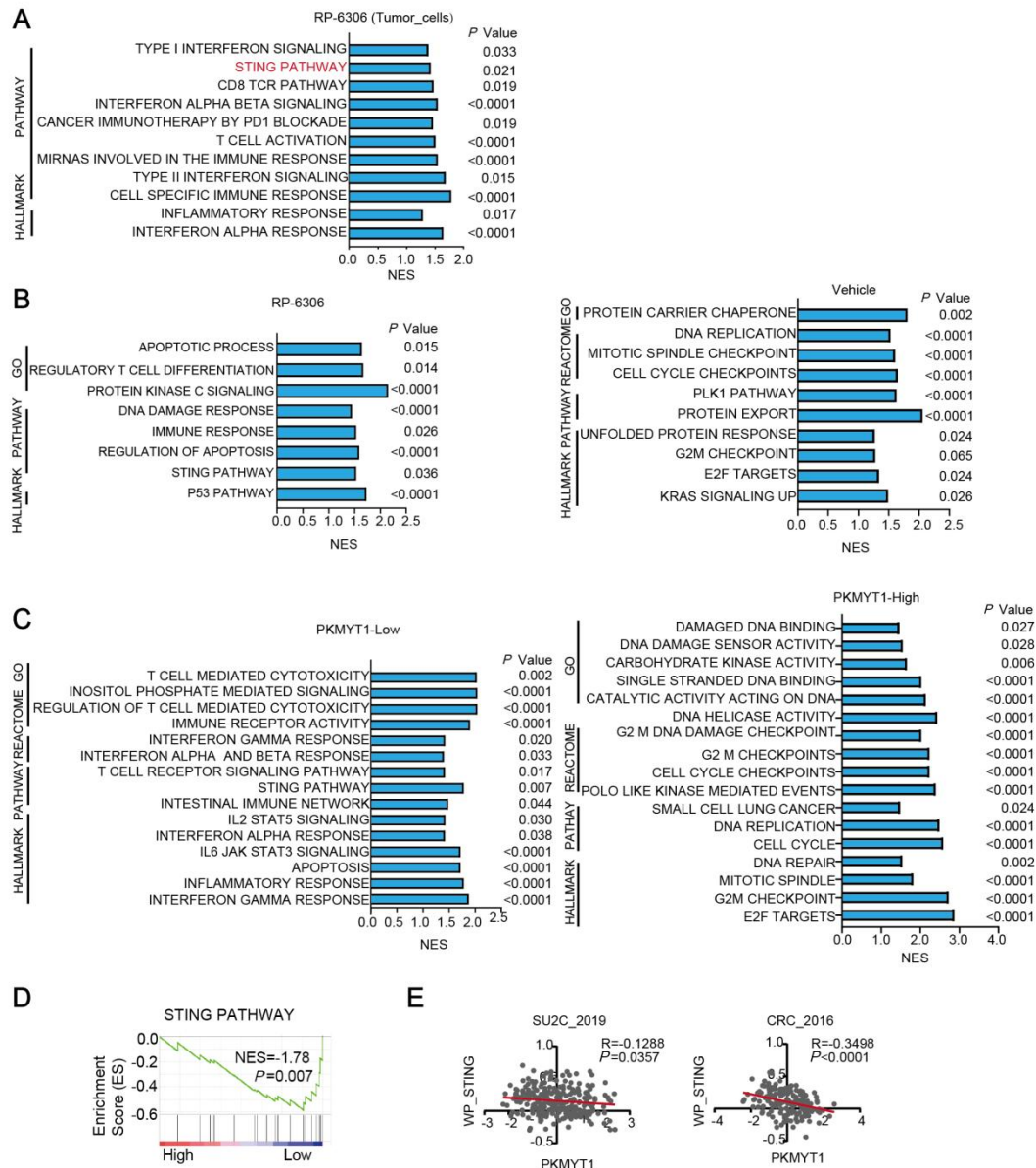
E. Representative images of dsDNA staining in indicated PCa cells transfected with siPKMYT1(left panel), and quantitative analysis of dsDNA staining in PCa cells with PKMYT1 knockdown (right panel). Data represent mean \pm SEM of three independent experiments. Scale bars, 10 μ m.

F-G. Images and the percentage of γ -H2AX positive cells in indicated cells with 5 μ M

RO-3306 and 500nM RP-6306 treatment for 24h. Scale bars, 20μm.

H. Images and the percentage of dsDNA positive cells in indicated cells with 5μM RO-3306 and 500nM RP-6306 treatment for 24h. Scale bars, 10μm.

* $P < 0.05$, *** $P < 0.001$, **** $P < 0.0001$.



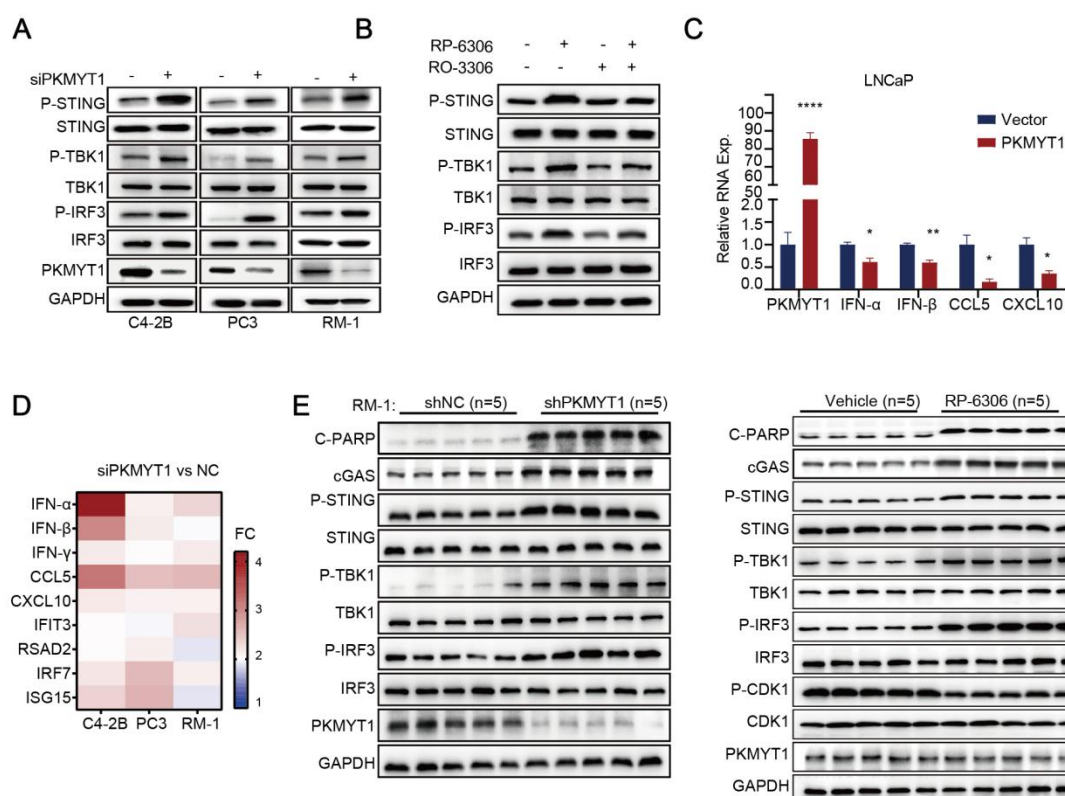
Supplementary Fig.6 PKMYT1-related signaling pathways in CRPC cells.

A. GSEA analysis of scRNA-seq profiles in epithelial cell cluster with RP-6306 treatment in RM-1 tumors.

B-C. GSEA of enriched gene sets in C4-2B cells treated with 500nM RP-6306 for 24h, and GSEA analysis from microarray datasets of GSE35988 that profiled CRPC cases with different levels of PKMYT1 expression. Gene sets from the Hallmark, KEGG, REACTOME and GO platforms were output by GSEA. NES, Normalized Enrichment Score.

D. Enrichment of STING pathway analyzed by GSEA in RNA-seq data for CRPC patients with PKMYT1 high and low expression in GSE35988 datasets.

E. The relationship between STING pathway signature and PKMYT1 expression in CRPC cases from SU2C-2019 and CRC-2016 datasets.



Supplementary Fig.7 PKMYT1 inhibition regulates the activity of STING signaling.

A. Western blots showing the protein expression of STING pathway, phosphorylated and total STING, TBK1, IRF3, and GAPDH (loading control) in indicated PCa cells with PKMYT1 knockdown.

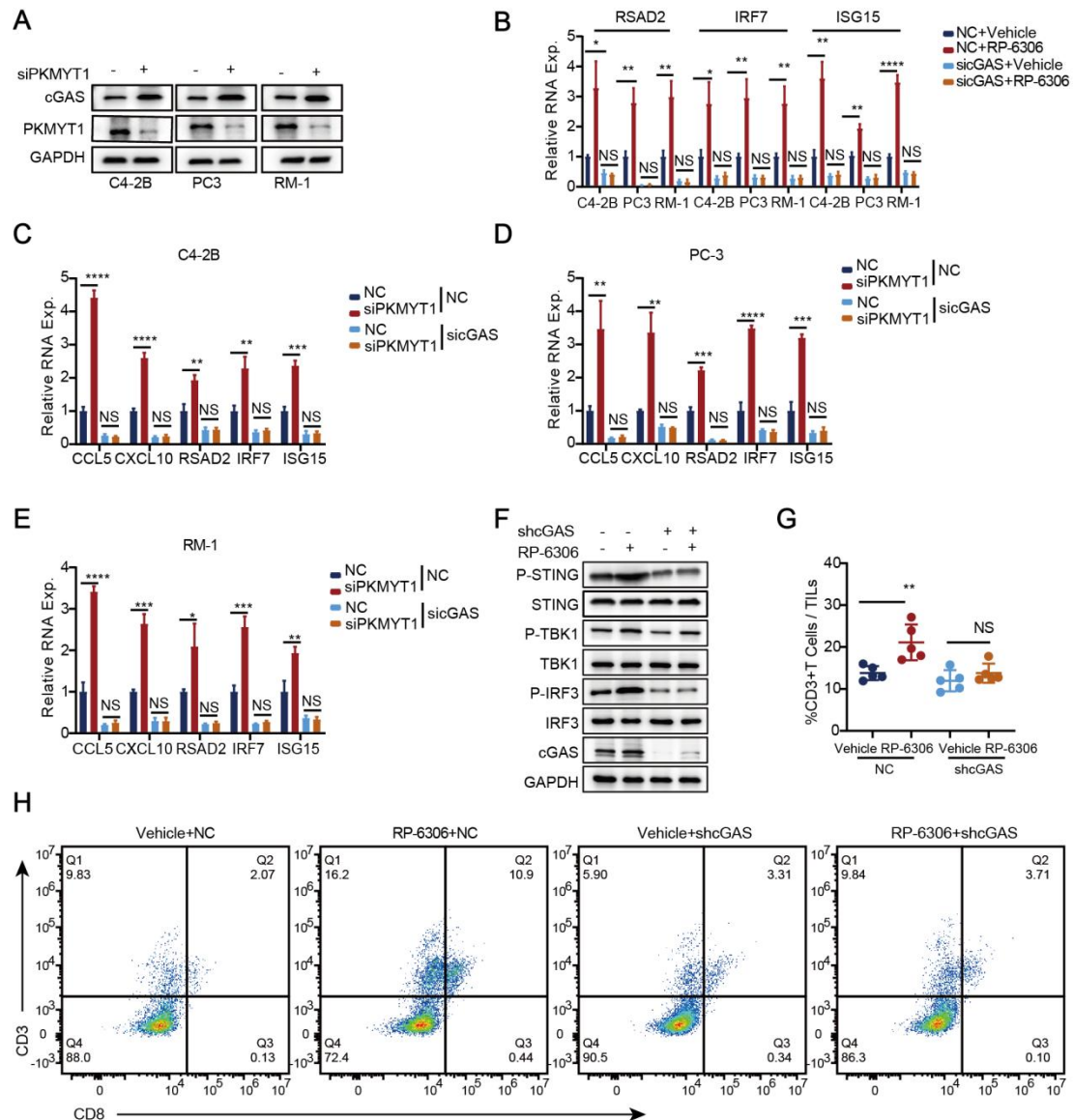
B. Western blots showing the protein expression of STING pathway in RM-1 cells with indicated treatment.

C. RT-qPCR analysis of IFN-α, IFN-β, CCL5 and CXCL10 in LNCaP cells expressed PKMYT1.

D. Fold changes of IFNs and ISGs expression levels in indicated PCa cells with PKMYT1 knockdown analyzed by RT-qPCR.

E. Expression of STING pathway related proteins in RM-1 tumors with indicated treatment. Tumors dissected from C57BL/6 mice bearing RM-1 cells, and subjected to protein extraction. The indicated protein expression levels were measured by western blot assays.

* $P < 0.05$, ** $P < 0.01$, *** $P < 0.001$, **** $P < 0.0001$.



Supplementary Fig.8 PKMYT1 inhibition regulates the activity of STING signaling in a cGAS-dependent manner.

A. Protein levels of cGAS in indicated PCa cells with PKMYT1 knockdown.

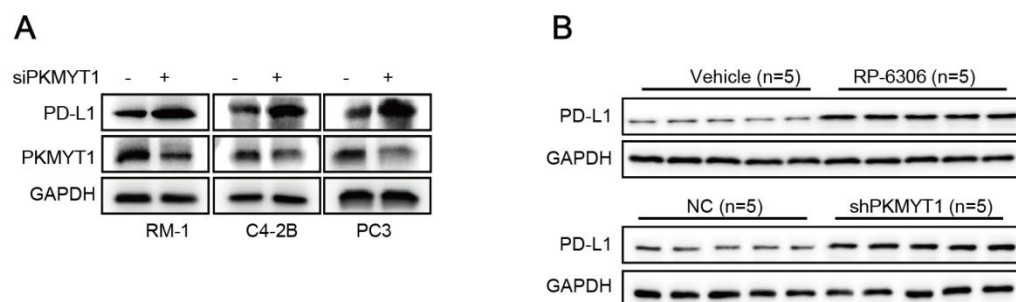
B-E. RT-qPCR analysis of ISGs levels in PCa cells with indicated treatment.

F. The protein expression levels of STING pathway measured western blot assays in RM-1 tumors with indicated treatment.

G. Percentage of CD3+ T cells in CD45+ T cells analyzed by flow-cytometry assays in RM-1 tumors. RM-1 tumors were harvested at day 10 for immune profiling by flow cytometry. Flow-cytometry analysis of CD45+CD3+ total T cells in the tumors are shown.

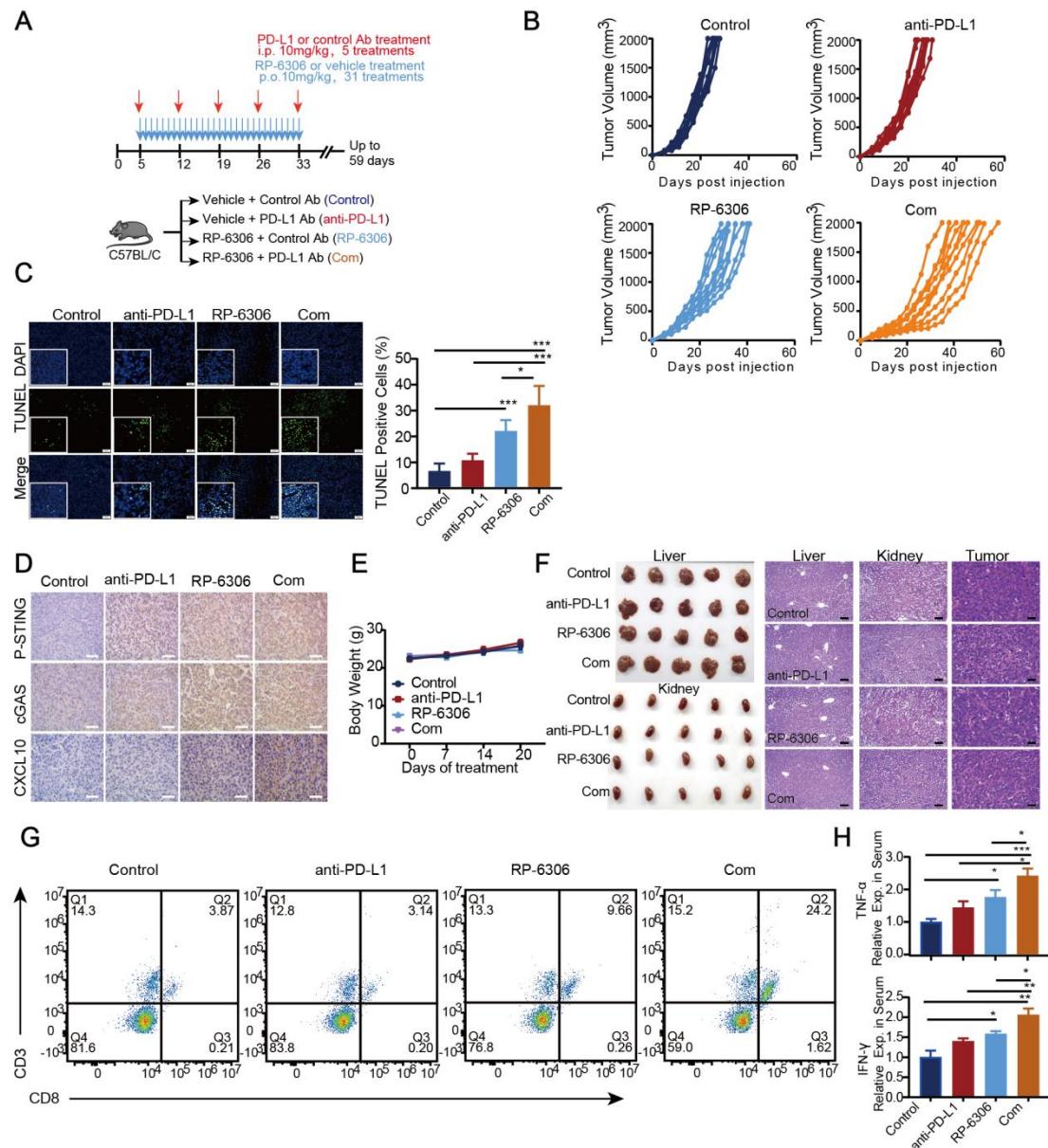
H. Images of CD8+ T cells analyzed by flow-cytometry assays in indicated RM-1 tumors.

* $P < 0.05$, ** $P < 0.01$, *** $P < 0.001$.



Supplementary Fig.9 PKMYT1 inhibition increases the protein expression of PD-L1.

A-B. PD-L1 expression analyzed by western blot assay in PCa cells and RM-1 tumors with indicated treatment.



Supplementary Fig.10 RP-6306 enhances the antitumor immune response to PD-L1 blockade in mouse model.

A. A schematic model that illustrated the treatment plan for mice bearing subcutaneous RM-1 tumors.

B. Tumor volumes of RM-1 syngeneic tumors treated with control (dark blue lines; n = 10), anti-mouse PD-L1 antibodies (red lines; n = 10), RP-6306 (light blue lines; n = 10), and combination of RP-6306 and anti-mouse PD-L1 antibodies (yellow lines; n = 10) plotted individually.

C. Images of TUNEL staining performed in RM-1 tumor tissues. Quantitative analysis of TUNEL staining in RM-1 tumors with indicated treatment were shown in right panel. Scale bars, 50μm.

D. Representative IHC images of P-STING, cGAS and CXCL10 in tumors in each group. Scale bars, 50μm.

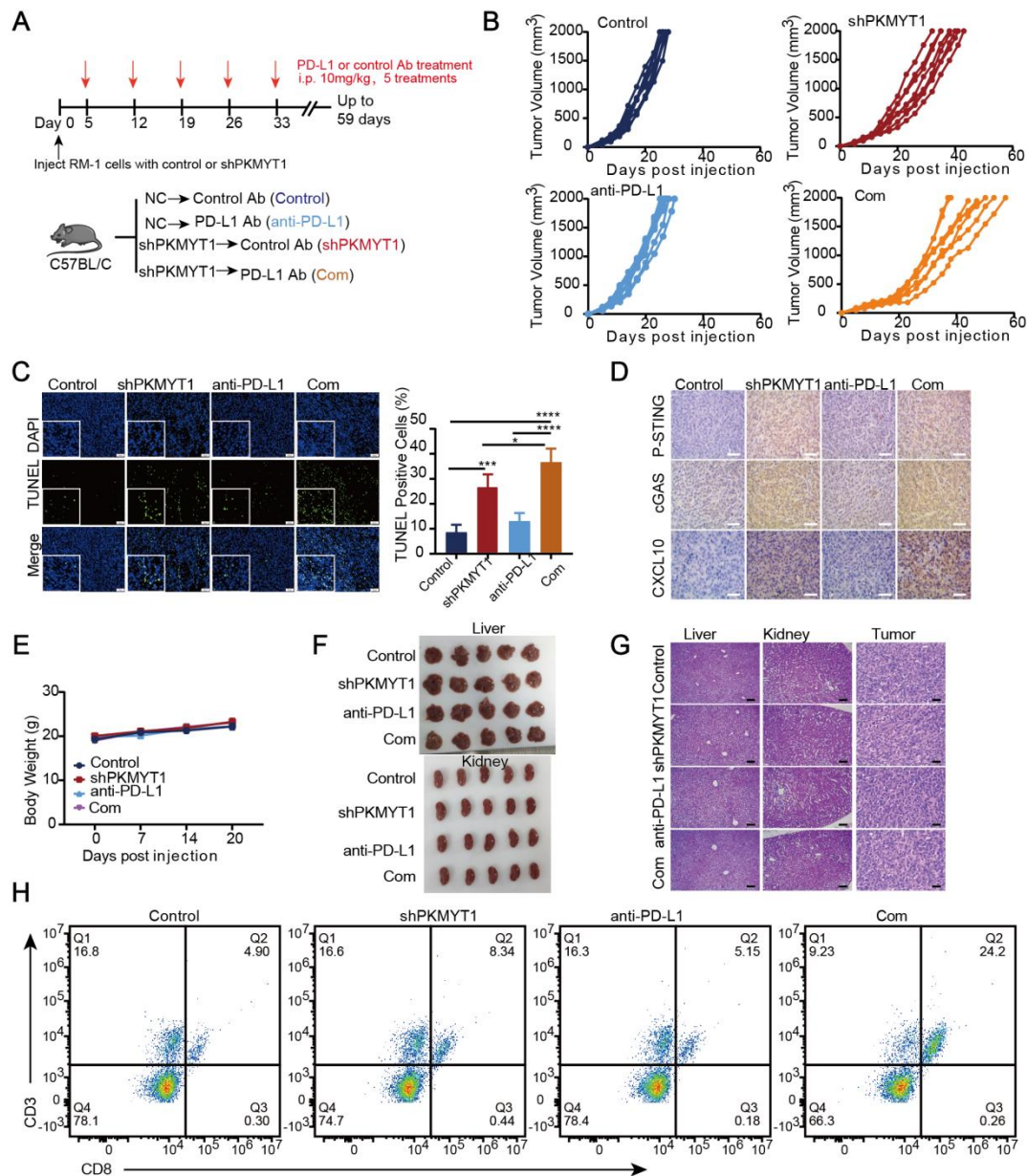
E. Body weight of RM-1 tumor-bearing mice in each group.

F. Drug toxicity in vital organs in each group. The livers and kidneys were photographed and stained with H/E in each group. Scale bars, 200 μ m.

G. Images of CD8⁺ T cells analyzed by flow-cytometry assays in indicated RM-1 tumors.

H. IFN- γ and TNF- α levels of serum analyzed by ELISA. Circulating serum from indicated C57BL/6 mice was analyzed for IFN- γ and TNF- α by cytokine ELISAs. The error bars indicate the mean \pm SEM of three independent assays.

* $P < 0.05$, ** $P < 0.01$, *** $P < 0.001$, **** $P < 0.0001$.



Supplementary Fig.11 PKMYT1 knockdown enhances the antitumor immune response to PD-L1 blockade in mouse model.

A. A schematic model that illustrated the treatment plan for mice bearing subcutaneous RM-1 tumors.

B. Tumor volumes of RM-1 syngeneic tumors treated with control (dark blue lines; n = 8), shPKMYT1 (red lines; n = 8), anti-mouse PD-L1 antibodies (light blue lines; n = 8), and combination of shPKMYT1 and anti-mouse PD-L1 antibodies (yellow lines; n = 8) plotted individually.

C. Images and quantitative analysis of TUNEL staining performed in RM-1 tumor tissues. Scale bars, 50μm.

D. Representative IHC images of P-STING, cGAS and CXCL10 in tumors in each group. Scale bars, 50μm.

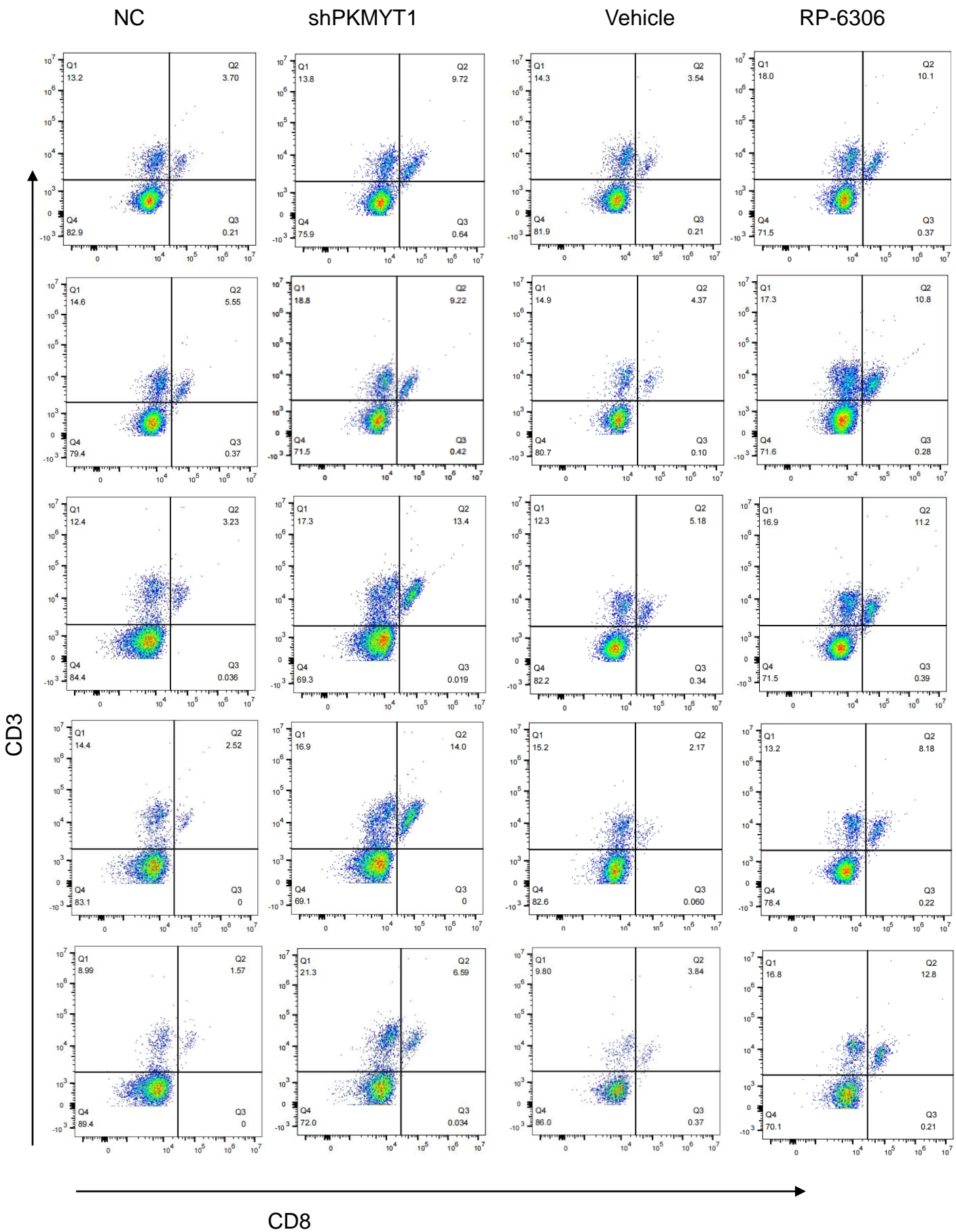
E. Body weight of RM-1 tumor-bearing mice in each group.

F-G. Drug toxicity in vital organs in each group. The livers and kidneys were photographed and stained with H/E in each group. Scale bars, 200 μ m.

H. Images of CD8⁺ T cells analyzed by flow-cytometry assays in indicated RM-1 tumors.

* $P < 0.05$, ** $P < 0.01$, *** $P < 0.001$, **** $P < 0.0001$.

Supplementary Fig.12 Images for the flow cytometry results.

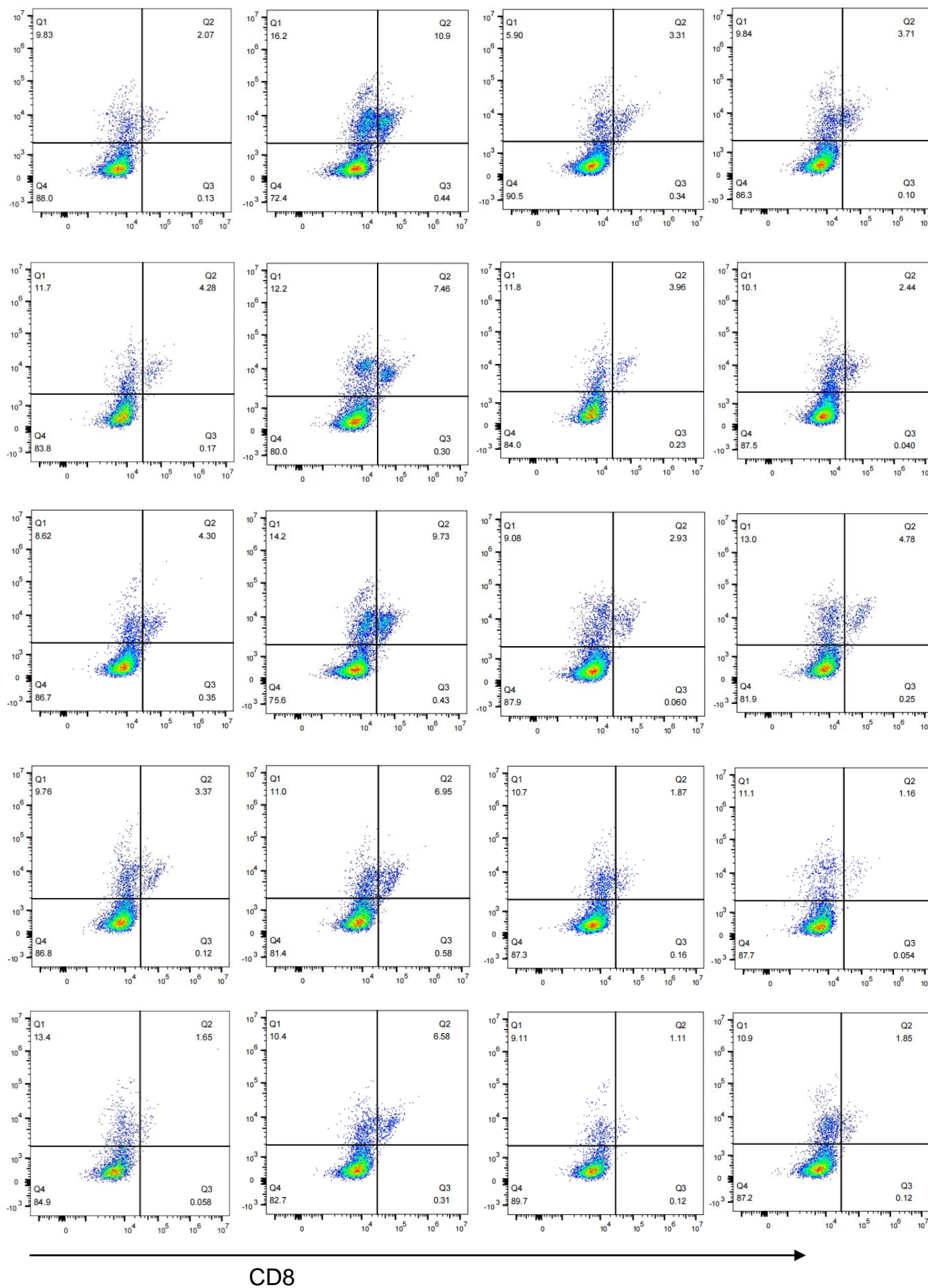


NC+Vehicle

NC+RP-6306

shcGAS+Vehicle

shcGAS+ RP-6306

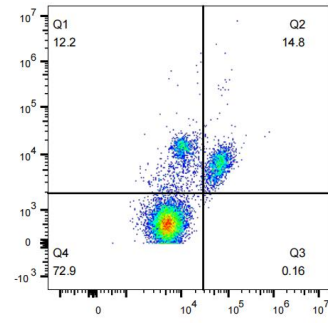
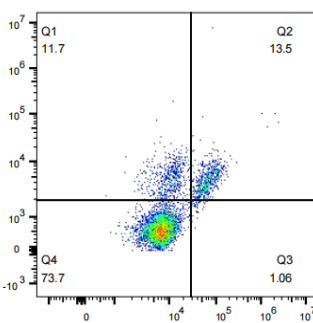
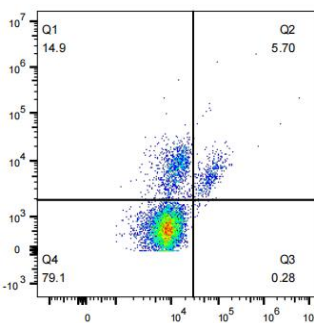
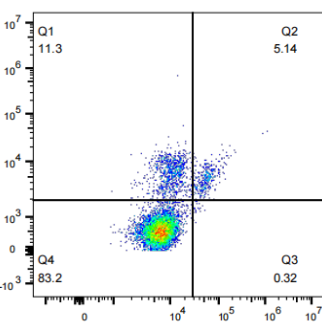
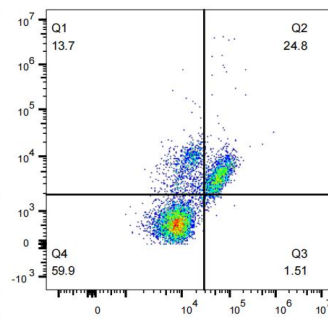
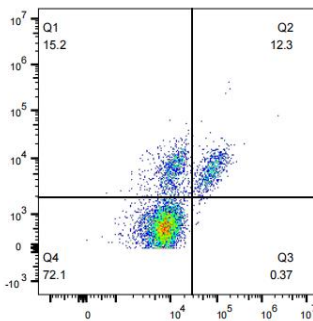
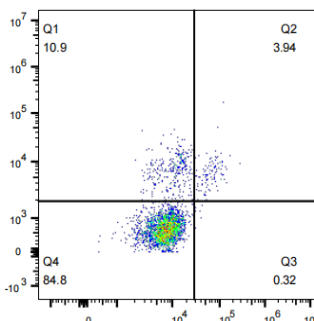
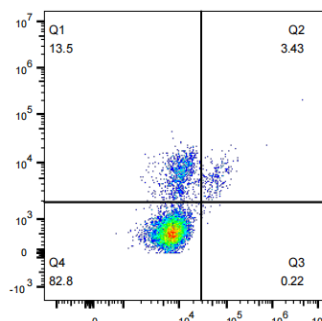
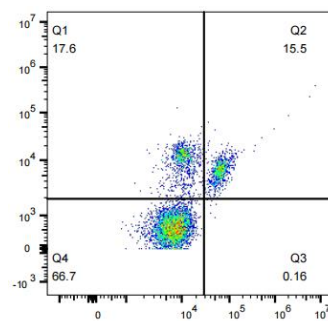
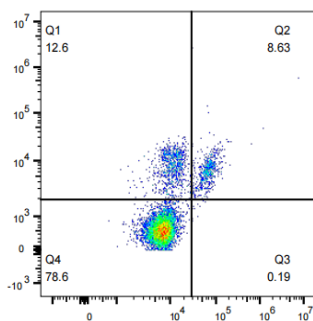
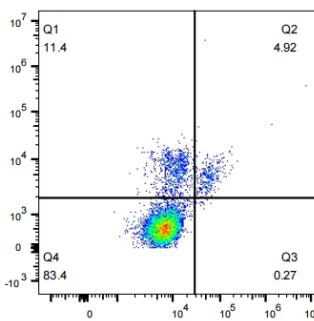
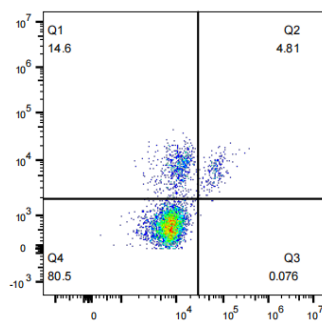
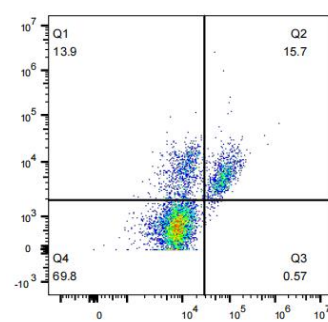
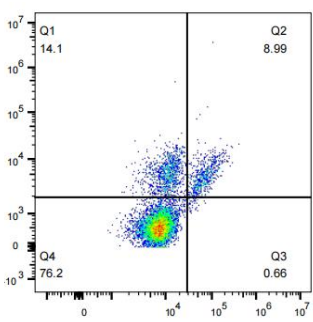
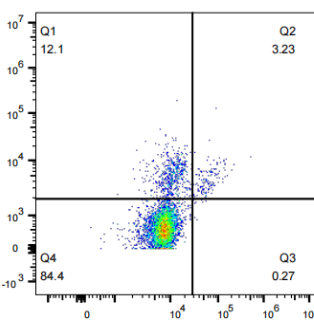
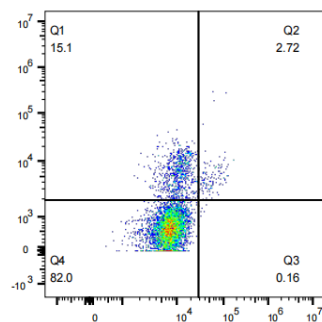
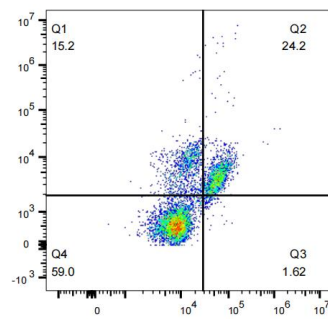
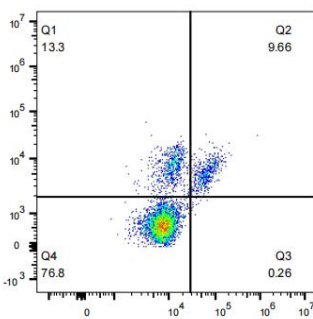
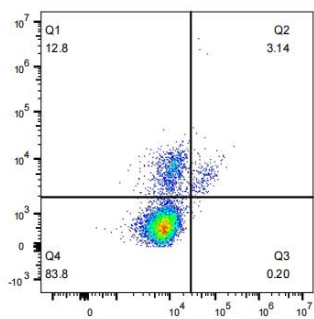
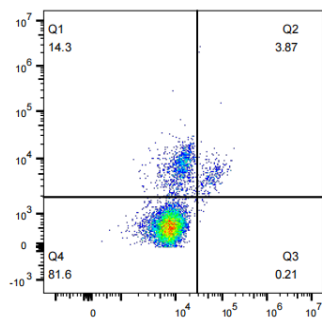


Control

anti-PD-L1

RP-6306

Com



CD3

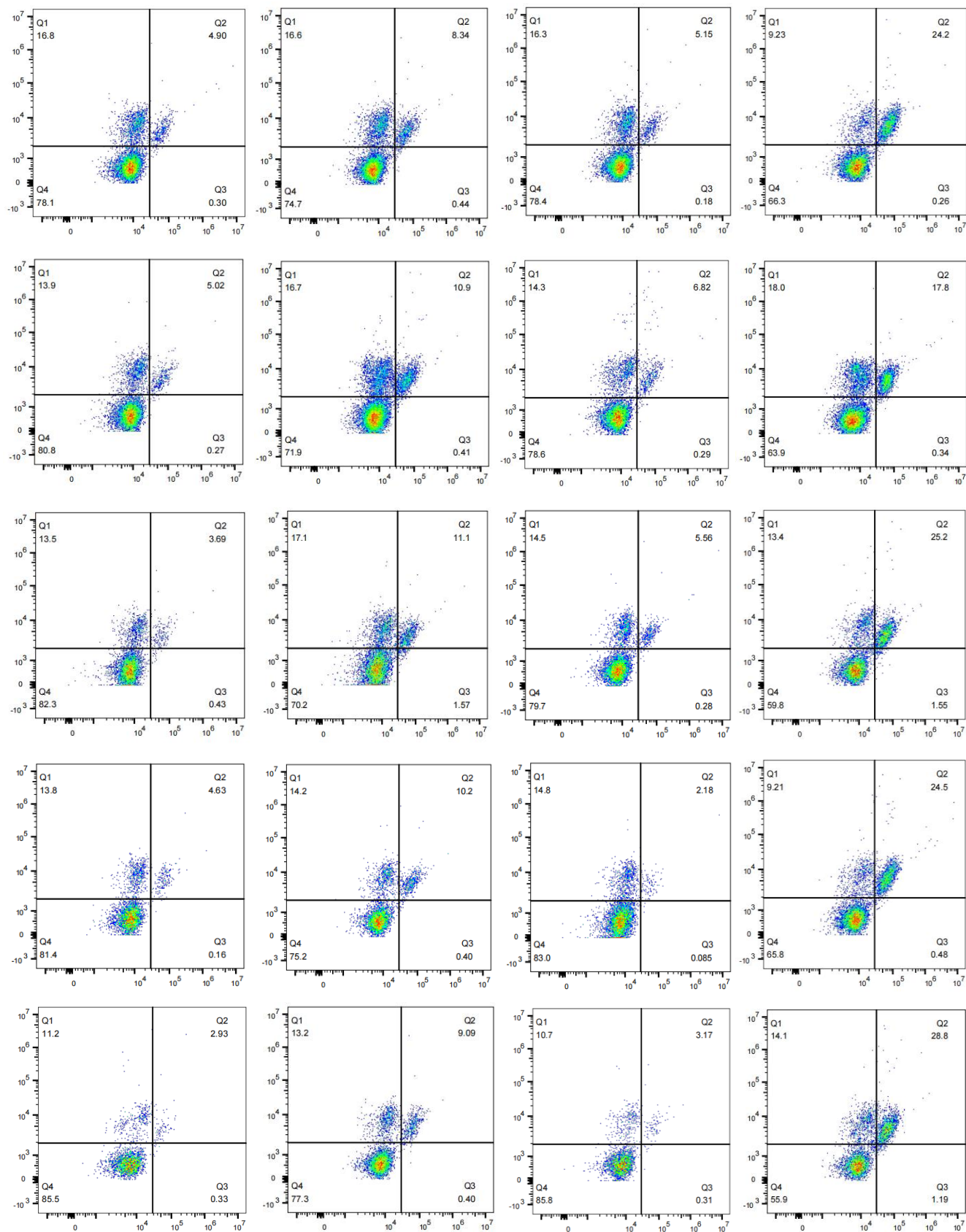
CD8

Control

shPKMYT1

anti-PD-L1

Com



CD8

Fig4E

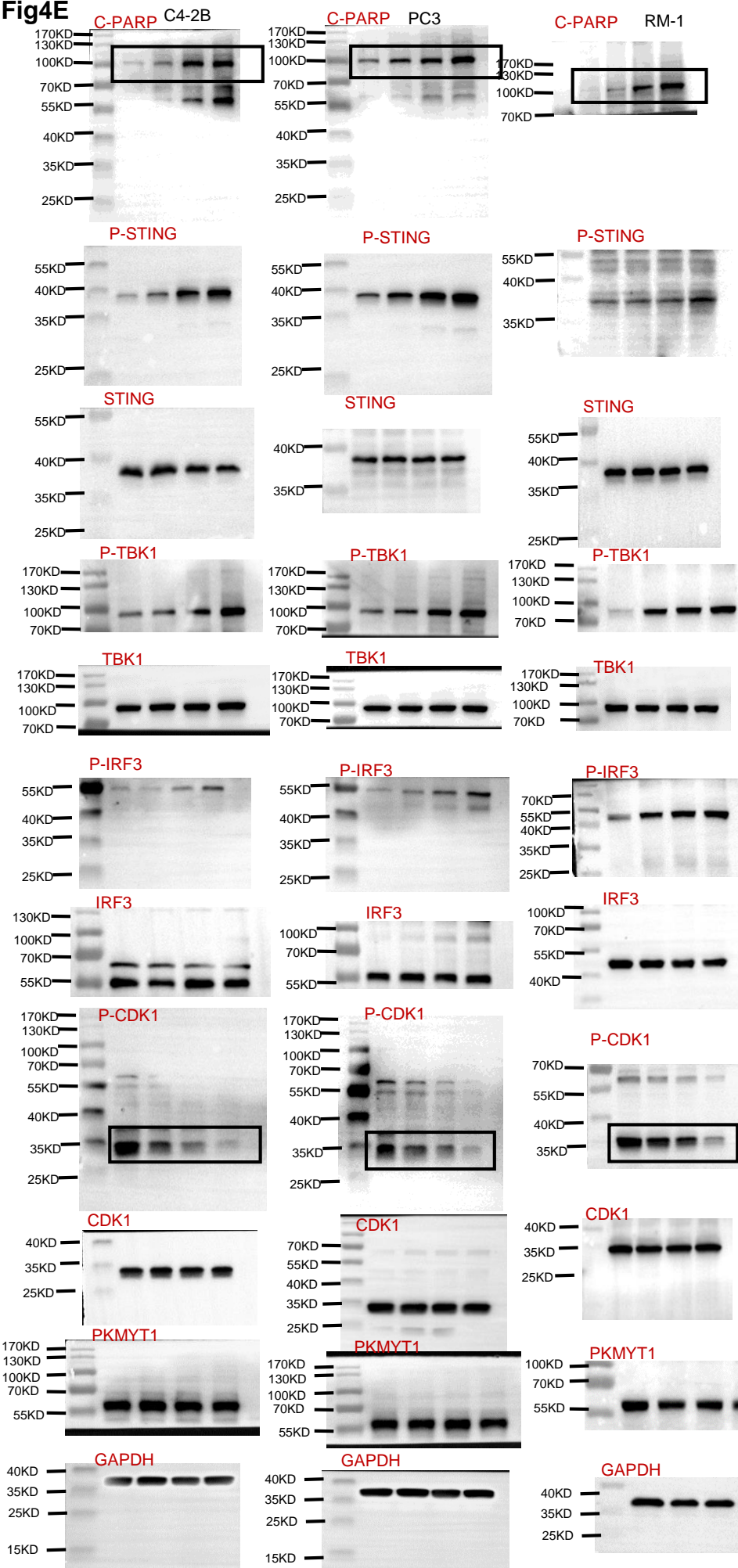


Fig4G

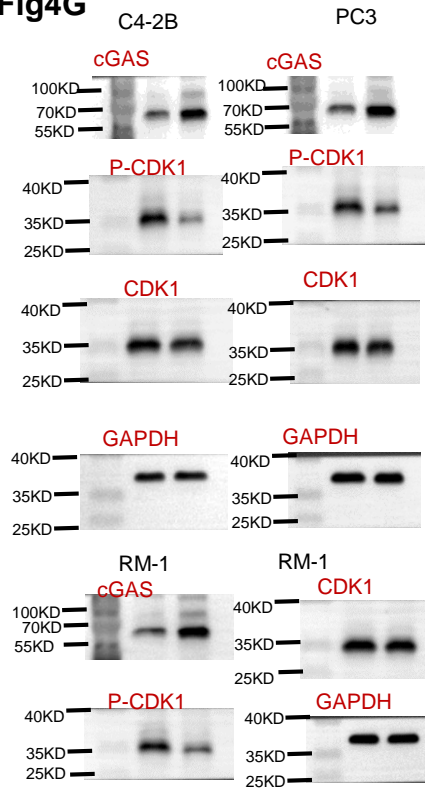


Fig4J

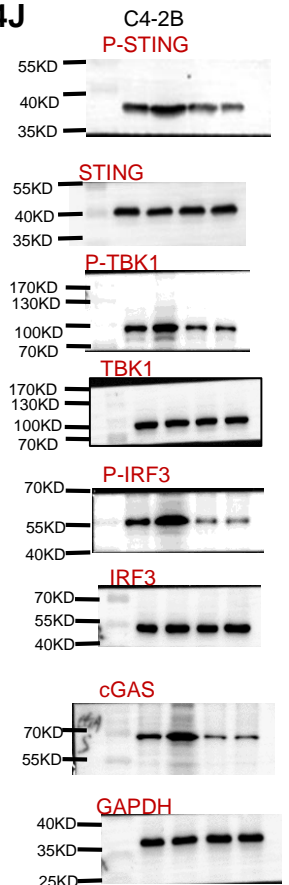
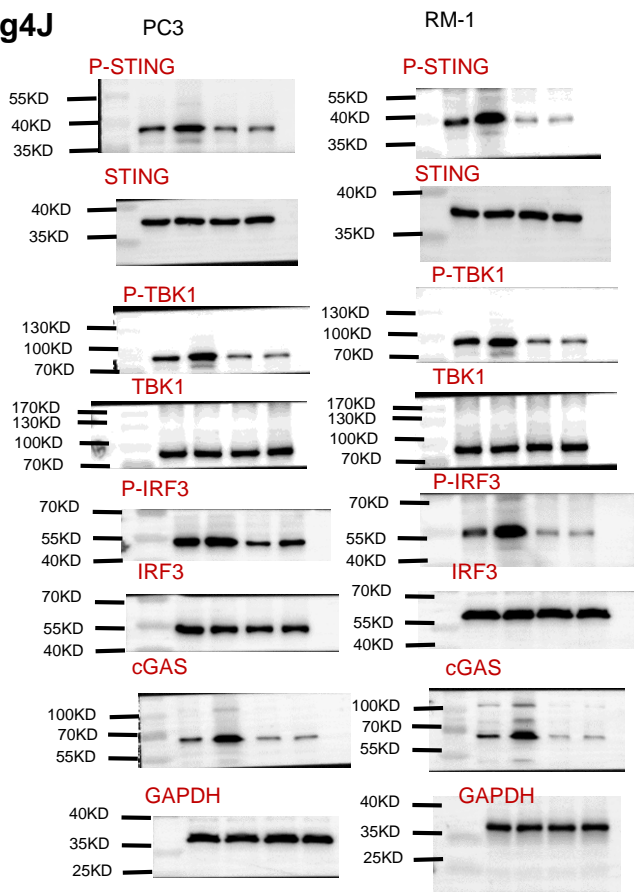
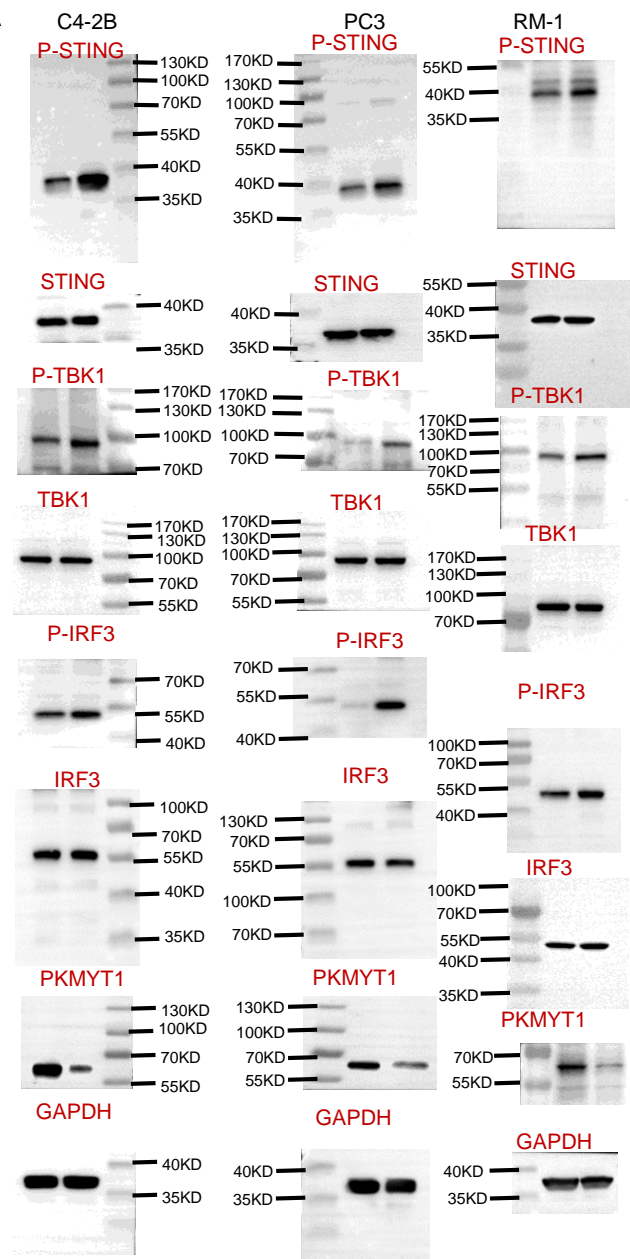
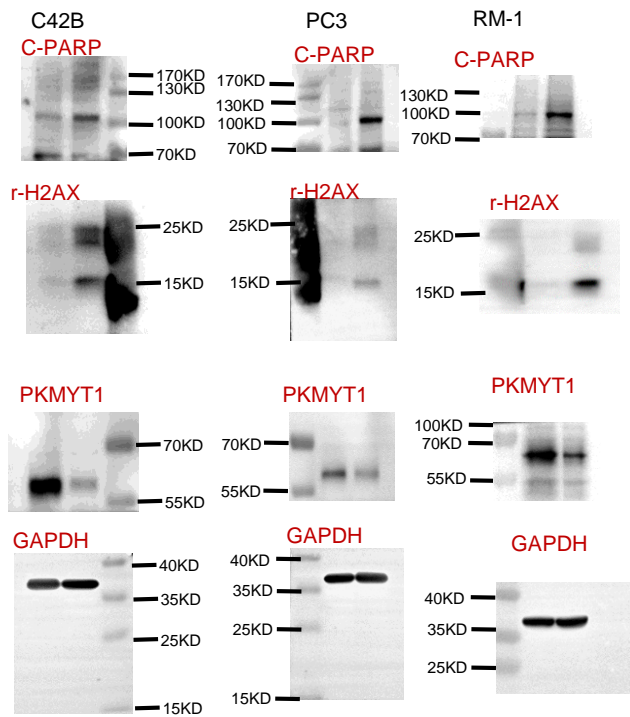
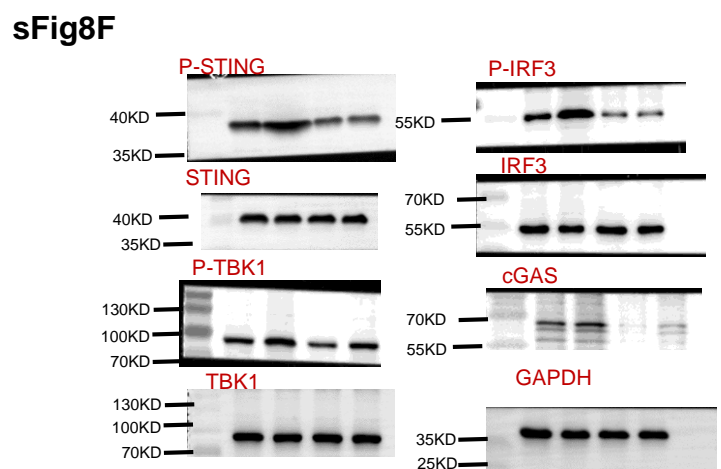
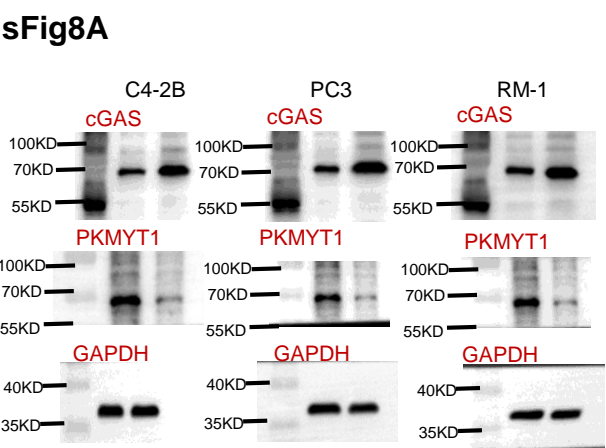
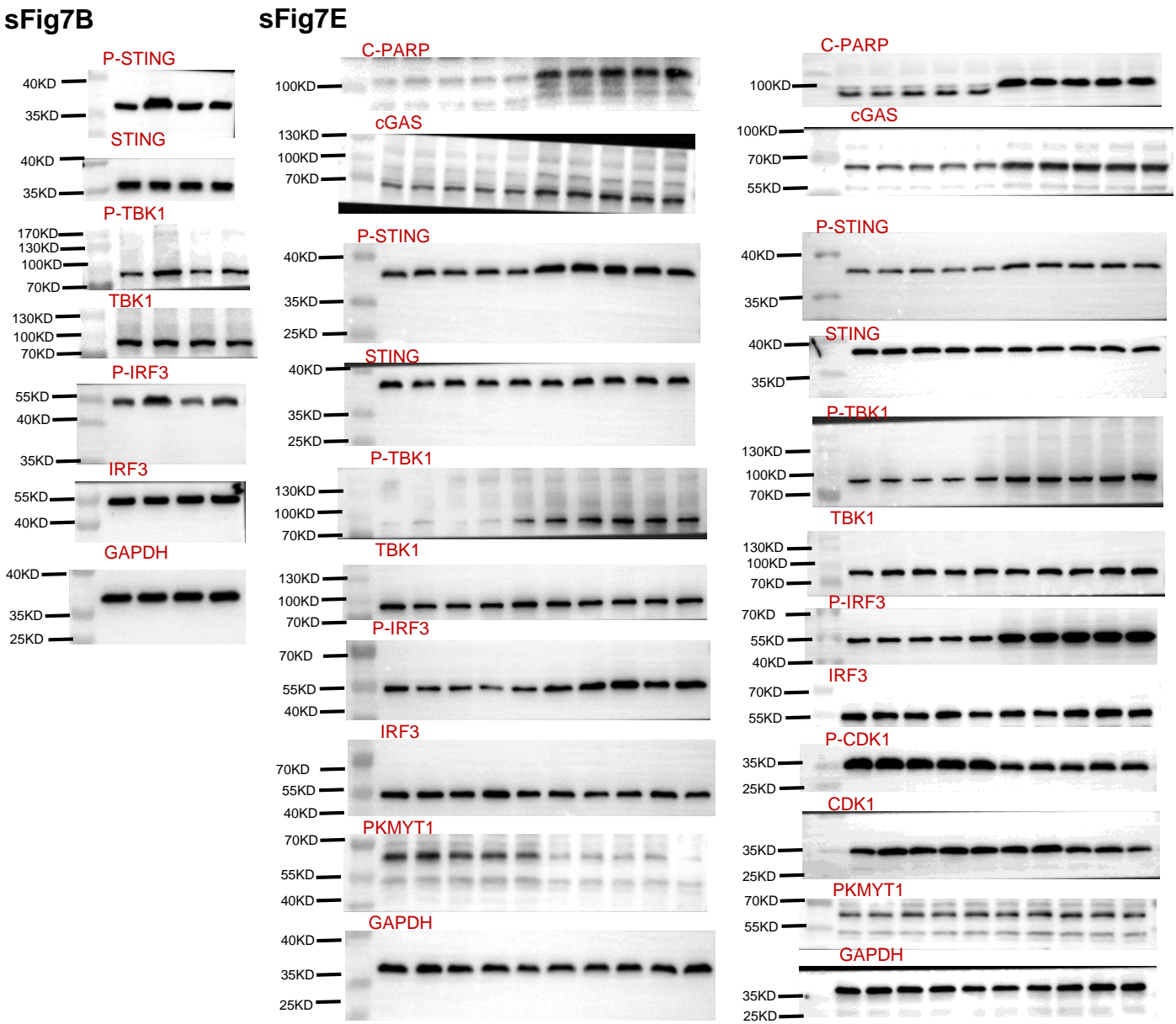
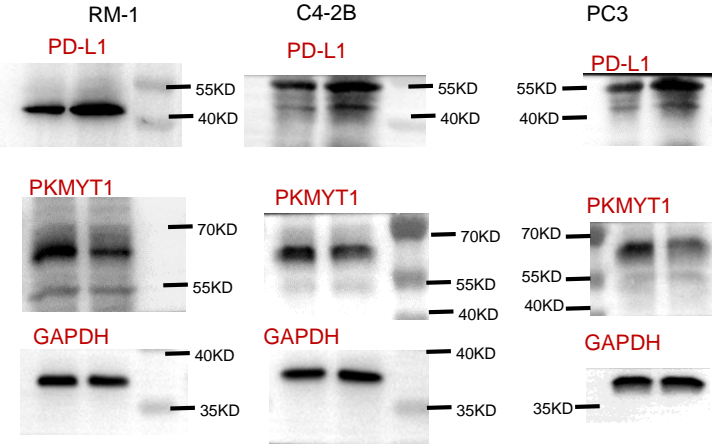


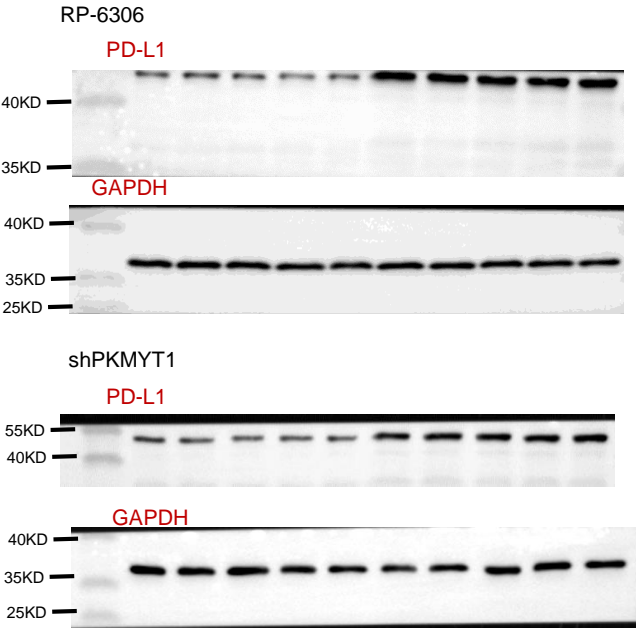
Fig4J**SFig7A****SFig5D**



sFig9A



sFig9B



Supplementary Table 1. Primers used in this study.

Gene	Forward	Reverse
human CCL5	TGCCCACATCAAGGAGTATTT	CTTTCGGGTGACAAAGACG
human CXCL10	GGCCATCAAGAATTTACTGAAAGCA	TCTGTGTGGTCCATCCTTGGA
human IFN-β	CAACTTGCTTGGATTCTACAAAG	TATTCAAGCCTCCCATTCAATTG
human GAPDH	GCACCGTCAAGGCTGAGAAC	TGGTGAAGACGCCAGTGGA
human IFN-α	GACTCCATCTTGGCTGTGA	TGATTTCTGCTCTGACAACCT
mouse Ifn-α	GGACTTTGGATTCCCGCAGGAGAAG	GCTGCATCAGACAGCCTTGCAGGTC
mouse Ifn-β	CAGCTCCAAGAAAGGACGAAC	GGCAGTGTAACCTCTTCTGCAT
mouse Ccl5	GCTGCTTTGCCTACCTCTCC	TCGAGTGACAAACACGACTGC
mouse Cxcl10	CCAAGTGCTGCCGTCATTTTC	GGCTCGCAGGGATGATTTCAA
mouse Pkmyt1	GTCTGTCTTCTGAGCTGCGT	CTCAGCATGGGTAAGGCCAA
human PKMYT1	ATGCTAGAACGGCCTCCTG	TTCTGCGTGGCGGAAGTAG
human IFN-γ	GAGTGTGGAGACCATCAAGGAAG	TGCTTTGCGTTGGACATTCAAGTC
mouse Ifn-γ	ATGAACGCTACACACTGCATC	CCATCCTTTTGCCAGTTCCCTC
human cGAS	TAACCCTGGCTTTGGAATCAAAA	TGGGTACAAGGTAAAATGGCTTT
mouse cgas	GTTCAAACACAAGAAATGCACTG	GCTGACGGAGTACACAATCCT
human IFIT3	AAAAGCCCAACAACCCAGAAT	CGTATTGGTTATCAGGACTCAGC
mouse Ifit3	TGAACTGCTCAGCCACA	TCCCGGTTGACCTCACTC
human ISG15	TGGACAAATGCGACGAACCTC	TCAGCCGTACCTCGTAGGTG
mouse Isg15	GGAACGAAAGGGGCCACAGCA	CCTCCATGGGCCTTCCCTCGA
human IRF7	GCACACACACATGCTGGACT	TTGGTTGGGACTGGATCTGC
mouse Irf7	TCCAGTTGATCCGCATAAGGT	CTTCCCTATTTTCCGTGGCTG
human RSAD2	CAGCGTCAACTATCACTTCACT	AACTCTACTTTGCAGAACCTCAC
mouse Rsad2	TGCTGGCTGAGAATAGCATTAGG	GCTGAGTGCTGTTCCCATCT
mouse Gapdh	AGGTCGGTGTGAACGGATTTG	TGTAGACCATGTAGTTGAGGTCA

These primers were purchased from Biosune Biotechnology (Shanghai, China).

Supplementary Table 2. Primary antibodies used in this study.

Primary antibodies	Company	Cat no.
P-STING	Cell Signaling Technology	19781
STING	Cell Signaling Technology	13647
P-STING(Ms)	Invitrogen	PA5-105674
P-TBK1	Cell Signaling Technology	5483
TBK1	Cell Signaling Technology	3504
P-IRF3	Cell Signaling Technology	4947
IRF3	Cell Signaling Technology	4302
P-CDK1	GeneTex	GTX133860
CDK1	Abways Technology	CY5061
CDK1(Ms)	Abways Technology	CY5177
PKMYT1	Cell Signaling Technology	4282
r-H2AX	Cell Signaling Technology	2577
GAPDH	Abways Technology	AB0037
c-PARP	Abways Technology	CY5265
c-PARP(Ms)	Abways Technology	CY5035
CD8	Cell Signaling Technology	70306
CD8(Ms)	Cell Signaling Technology	98941
cGAS	Proteintech	29958-1-AP
PD-L1	Proteintech	17952-1-AP
CCL5	Invitrogen	710001
CXCL10	Proteintech	10937-1-AP

Supplementary Table 3. siRNAs used in this study.

siRNA	Sequence
siPKMYT1	GUGACAUCAACUCAGAGCCTT
siPKMYT1 (Ms)	GGCTCTGGACCATCTACATAG
siGAS	CGUGAAGAUUUCUGCACCU
siGAS (Ms)	GGCCGAGACGGUGAAUAAATT
shNC	GTTCTCCGAACGTGTCACGT
shPKMYT1	GTGACATCAACTCAGAGCC
shGAS	CCTCTTTAGGATTGTCAGAAT

These siRNA were purchased from GenePharma (Shanghai, China).

Supplementary Table 4. Gene list used for GSEA.

HALLMARK_INFLAMMATORY_RESPONSE,
REACTOM_INTERFERON_ALPHA_BETA_SIGNALING, STING pathways, et al. were obtained
from GSEA (<http://software.broadinstitute.org/gsea/index.jsp>).
PKMYT1_SIGNATURE were TOP200 positive related to PKMYT1 expression in PCa obtained
from GEPIA database.

PKMYT1_SIGNATURE (200)				
CHTF18	TK1	AC005606.15	RP11-178L8.8	RP11-671J11.5
POLD1	RP4-738P15.6	WDR34	EDF1	CTD-2540B15.11
SAC3D1	CDC20	NCAPH2	SKIV2L	PTTG1
SPC24	INTS1	HRAS	TRAIP	CDK5RAP3
CEMP1	H2AFX	ABCB6	DNAJC7	AC005943.6
NUP85	WDR46	MAP1S	ZNF317	CTB-43P18.1
RP11-386G11.10	EEF1D	SART1	RP13-131K19.2	UQCC3
SPAG5	GFER	NSUN5P2	TMEM160	RPL35
PSMG3	RP11-661A12.8	RP11-548H3.1	CITF22-1A6.3	METTL12
RP11-256P1.1	NMRAL1	NAT14	RBM6	AC005339.2
NUDT1	RNF31	POLE	RP11-161H23.5	AC074212.5
ARAP1-AS1	AURKAIP1	ORAOV1	GP1BB	ROMO1
BOLA2B	C16orf59	ARMCX7P	C6orf136	CTB-129O4.1
POLRMT	FANCA	RP11-6N17.6	CDC34	RP11-304L19.13
C9orf142	AURKB	RP11-63M22.2	NDUFB11	RP11-360L9.7
DDX56	MAP2K2	SULT1A3	NDUFB7	BCL7C
C14orf80	RPL28	POLR2I	AP003068.9	DPP7
BUD31	WDR13	TACC3	AC005306.3	COX6B1
RP11-498C9.13	AC006547.8	MRPS34	NME3	SYMPK
LIG1	TYK2	CPSF1	TUBGCP2	RP11-307C12.12
FAM195A	HCG25	SLC4A2	ABHD16B	FAM50A
C19orf43	AC007192.6	STUB1	LRRC45	ATP5D
AC007308.7	CTD-2589H19.6	ATP5I	RPP21	CEP131
LAMTOR4	BRICD5	RP11-498P14.3	C19orf60	C16orf13
CTB-31O20.3	RP11-368P15.3	RP1-20B21.4	NUP214	RPL37P6
RP11-109P14.10	DROSHA	TCEB2	RP11-16E23.5	RP11-264B17.2
RPLP2	RP11-618K13.2	RP11-566K11.5	AC110615.1	C20orf27
C17orf89	ARL6IP4	SNRPA	PPP1R35	RP11-114H24.6
SNRPD2	RAD54L	RP11-574K11.32	AC104534.3	MRPL23
FANCG	COMTD1	RP11-697E22.1	PSMB3	CTD-2636A23.2
AL513523.2	ZNHIT1	CTC-273B12.5	RP13-39P12.3	RP11-746M1.1
LSM7	LINC01176	RPS19	SFXN4	MRPL38
AP001615.9	C19orf24	CTC-1337H24.4	EIF3C	RP3-508I15.18
RP11-638I2.6	SIGIRR	SUPV3L1	AC006011.4	CTD-2510F5.6
GADD45GIP1	IRF3	PAM16	CDCA3	LA16c-390E6.5
DDX49	LAGE3	QTRT1	CCDC85B	ITPA
RP11-667K14.4	E2F1	NAA10	RP11-298I3.5	GMPSP1
MXD3	RP11-756A22.7	DNAJC9-AS1	PRR14	RP11-867G23.4
RFXANK	NKX6-2	MICALL2	PNPLA6	ASPSCR1
TSEN54	MIIP	PET100	ZBTB48	CDC45